A Novel, Tunable Manganese Coordination System Based on a Flexible "Spacer" Unit: Noncovalent Templation Effects

Frank M. Tabellion, S. Russell Seidel, Atta M. Arif, and Peter J. Stang*

Contribution from the Department of Chemistry, University of Utah, 315 South 1400 East, Room 2020, Salt Lake City, Utah 84112

Received June 11, 2001

Abstract: The reaction of bis(hexafluoroacetylacetonato)manganese(II) trihydrate (**2**), an ∼90° corner unit, with flexible linking unit 4,4′-trimethylenedipyridine (**1**) allows for the potential formation of three different types of solid-state coordination species: infinite helical polymers, closed dimeric systems, and infinite one-dimensional polymers. While the un-templated starting material is known to give a coordination helix, the other two possible species can be realized through the selective use of a variety of simple, organic guests: toluene (**3**), diphenylmethane (**4**), *cis*-stilbene (**5**), 1,3-diphenylpropane (**6**), benzyl alcohol (**7**), nitrobenzene (**8**), and cyanobenzene (**9**). When solutions of **1** and **2** are crystallized in the presence of all of these clathrates, the dimeric macrocycles result in all cases, except for that of **6**, in which a syndiotactic, wedge-shaped polymer forms. Employing a linker that is less rigid than is typically used in crystal engineering, such as **1**, enables the nucleophilic donor subunit to be more than just a simple "spacer", instead making it an essential, tunable component in the overall crystal lattice. In so doing, a great deal of molecular "information" is lost, but this is compensated for by an in-depth investigation into the weaker host−guest and/or guest−guest interactions, such as nonclassical hydrogen bonding and an assortment of hydrophobic interactions, present in the various systems.

Introduction

Supramolecular architecture, comprising both inorganic crystal engineering (ICE)[1] and discrete molecular assembly (DMA),[2] has emerged as an innovative area at the forefront of modern day chemistry. While DMA focuses on the synthesis of distinct entities formed and characterized primarily in solution, ICE is centered solely on functionalizing the solid state. The most intriguing aspect of the latter is the notion of one day being able to manipulate not only the features of specific molecules, but also the bulk, intermolecular characteristics and properties of the entire crystalline aggregate.[1a] Driving this field forward are a variety of potential applications, such as host−guest chemistry, micro/mesoporous materials, and relevance to catalysis and molecular electronics/optoelectronics and devices. To date, a plethora of eloquent research has been conducted in this discipline, resulting in an extensive array of helices[3] and one-dimensional coordination polymers, two-dimensional grids, and three-dimensional lattices.[1] Typically, these coordination-based systems employ di- or multitopic metal centers and rigid, organic subunits or "spacers". The most common strategy relies upon the proper programming of angular and dimensional information into both the electrophilic metals and the nucleophilic "spacers". In so doing, the topology of the ensuing product can be reasonably controlled and directed. Other intermolecular interactions, such as $\pi-\pi$ stacking[4] and hydrogen bonding,[1h,5] can also be utilized in the "encoding" phase to give an extra handle on regulating the crystallization process.

One drawback that every contemporary "crystal engineer" faces arises from the tendency of such systems to self-intercalate, thereby reducing the accessible pore/cavity size and the predictability. Several tactics have proven useful in precluding interpenetration, including the appropriate choice of counterion[6]

(1) (a) Robson, R. In *Comprehensive Supramolecular Chemistry*; Atwood, J. L., Davies, J. E. D., MacNicol, D. D., Vögtle, F., Lehn, J.-M., Eds.; Pergamon: Oxford, UK, 1997; Vol. 6, pp 733−755. (b) Goodgame, D. M. L.; Menzer, S.; Smith, A. M.; Williams, D. J. *J. Chem. Soc., Dalton Trans.* **1997**, 3213−3218. (c) Yaghi, O. M.; Davis, C. E.; Li, G.; Li, H. *J. Am. Chem. Soc.* **1997**, *119*, 2861−2868. (d) Zaworotko, M. J. *Chem. Soc. Rev.* **1994**, *23*, 283−288. (e) Hirsch, K. A.; Wilson, S. C.; Moore, J. S. *Chem. Eur. J.* **1997**, *3*, 765−771. (f) Robson, R. *J. Chem. Soc., Dalton Trans.* **2000**, 3735−3744. (g) Hagrman, P. J.; Hagrman, D.; Zubieta, J. *Angew. Chem., Int. Ed. Engl.* **1999**, *38*, 2638−2684. (h) Braga, D.; Grepioni, F.; Desiraju, G. R. *Chem. Rev.* **1998**, *98*, 1375−1405. (i) Braga, D. *J. Chem. Soc., Dalton Trans.* **2000**, 3705−3713. (j) Eddaoudi, M.; Moler, D. B.; Li, H.; Chen, B.; Reineke, T. M.; O'Keeffe, M.; Yaghi, O. M. *Acc. Chem. Res.* **2001**, *34*, 319−330.

(2) (a) Lehn, J.-M. *Supramolecular Chemistry Concepts and Perspectives*; VCH: Weinheim, 1995; pp 139−160. (b) Swiegers, G. F.; Malefetse, T. J. *Chem. Rev.* **2000**, *100*, 3483−3538. (c) Chambron, J.-C.; Dietrich-Buchecker, C.; Sauvage, J.-P. In *Comprehensive Supramolecular Chemistry*; Lehn, J.-M., Atwood, J. L., Davies, J. E. D., MacNicol, D. D., Vögtle, F., Eds.; Pergamon: Oxford, UK, 1996; Vol. 9, pp 43−83. (d) Caulder, D. L.; Raymond, K. N. *Acc. Chem. Res.* **1999**, *32*, 975−982. (e) Caulder, D. L.; Raymond, K. N. *J. Chem. Soc., Dalton Trans.* **1999**, *8*, 1185−1200. (f) Fujita, M. *Chem. Soc. Rev.* **1998**, *6*, 417−425. (g) Leininger, S.; Olenyuk, B.; Stang, P. J. *Chem. Rev.* **2000**, *100*, 853−908. (h) Uller, E.; Demleitner, B.; Bernt, I.; Saalfrank, R. W. In *Structure and Bonding*; Fujita, M., Eds.; Springer: Berlin, 2000; Vol. 96, pp 149−175.

(3) (a) Piguet, C.; Bernardinelli, G.; Hopfgartner, G. *Chem. Rev.* **1997**, *97*, 2005−2062. (b) Hasenknopf, B.; Lehn, J.-M.; Boumediene, N.; Dupont-Gervais, A.; van Dorsselaer, A.; Kneisel, B.; Fenske, D. *J. Am. Chem. Soc.* **1997**, *119*, 10956−10962. (c) Tabellion, F. M.; Seidel, S. R.; Arif, A. M.; Stang, P. J. *Angew. Chem., Int. Ed. Engl.* **2001**, *40*, 1529−1532.

(4) (a) Janiak, C. *J. Chem. Soc., Dalton Trans.* **2000**, 3885−3896. (b) Alcock, N. W.; Barker, P. R.; Haider, J. M.; Hannon, M. J.; Painting, C. L.; Pikramenou, Z.; Plummer, E. A.; Rissanen, K.; Saarenketo, P. *J. Chem. Soc., Dalton Trans.* **2000**, 1447−1462.

(5) (a) Desiraju, G. R. *J. Chem. Soc., Dalton Trans.* **2000**, 3745−3751. (b) Miller, H. A.; Laing, N.; Parsons, S.; Parkin, A.; Tasker, P. A.; White, D. J. *J. Chem. Soc., Dalton Trans.* **2000**, 3773−3782. (c) Brammer, L.; Rivas, J. C. M.; Atencio, R.; Fang, S.; Pigge, F. C. *J. Chem. Soc., Dalton Trans.* **2000**, 3855−3867.

(6) Noro, S.; Kitagawa, S.; Kondo, M.; Seki, K. *Angew. Chem., Int. Ed. Engl.* **2000**, *39*, 2082−2084.

10.1021/ja0114310 CCC: $20.00
Published on Web 11/07/2001

Chart 1. Schematic Representation of the Three Reasonable Outcomes of Reacting Donor Linker **1** with Acceptor Complex **2**

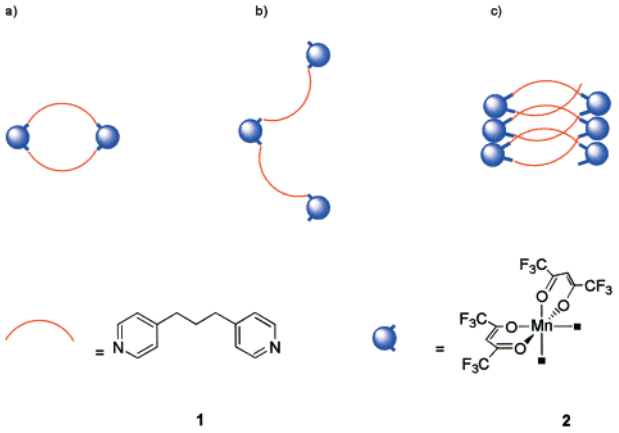

and the use of large secondary building blocks.[7] Of particular relevance are recent results by both Fujita[8] and Zoworotko,[9] wherein self-inclusion is prevented by exploiting noncovalently bound organic guests as place-holders in the overall lattice.

Here, we present a novel approach to crystal engineering, in which a single metal−ligand system provides the foundation for an assortment of different solid state arrangements. To realize this goal, the widely held belief that the nucleophilic subunits are merely "spacers" should be rethought. Instead, they have to be viewed as essential, tunable components of the overall architecture. This can be accomplished by employing a less rigid donor linker. Concomitantly, however, a considerable amount of the pre-programmed information that serves as a basis for product predictability is lost. We compensate for this by the inclusion of a wide array of simple, organic templates and guests into the crystal lattice. Not only can such species play an integral role in the solid state assembly process itself, but they can also provide a means for prohibiting framework interpenetration.

Flexible 4,4′-trimethylenedipyridine (1,3-bpyp, **1**) and bis-(hexafluoroacetylacetonato)manganese(II) trihydrate (**2**), a ditopic ∼90° corner,[10] fulfill the requisite criteria well. The crystallization of this metal−ligand combination can give rise to three logical structural designs: (a) a closed dimeric system; (b) an infinite, one-dimensional polymer; and (c) an infinite helical polymer (Chart 1).

Herein, we present the first comprehensive overview of this system, in which various organic clathrates have a profound influence on the entire crystal-topology and, to a large degree, disallow self-intercalation. As suitable aromatic guests, toluene (**3**), diphenylmethane (**4**), *cis*-stilbene (**5**), and 1,3-diphenylpropane (**6**) are used (Chart 2).

Such species are capable of hydrophobic/hydrophilic interactions and face-to-face/edge-to-face π interactions. In addition to this, benzyl alcohol (**7**), nitrobenzene (**8**), and cyanobenzene (**9**) are exploited for their relatively high polarity, and the potential aromatic C−H···O/C−H···N weak hydrogen-bonding interactions that this could incur.[8,11]

Chart 2. Nonpolar, **3**−**6**, and Polar, **7**−**9**, Organic Clathrates Utilized

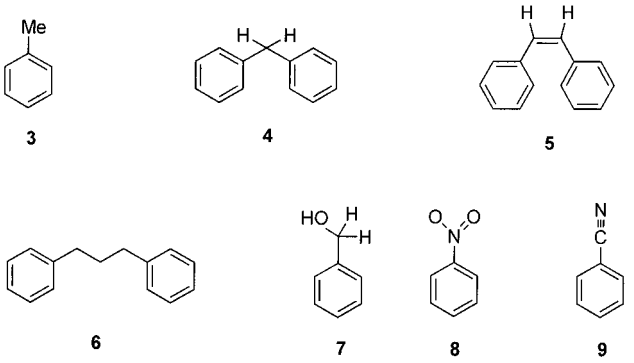

Experimental Section

General. All materials were used as received from commercial sources (Sigma-Aldrich or Lancaster).

Preparation of [Mn(hfacac)$_2$(1,3-bpyp)]$_2$·(toluene) (10). Slow evaporation of an acetone/hexanes solution of 61.7 mg (0.311 mmol) of **1** and 162.9 mg (0.311 mmol) of **2** in the presence of **3** gave 213.7 mg (96%; yellow solid) of **10**. Calculated for $Mn_2C_{53}H_{40}N_4O_8F_{24}$: C 44.62, H 2.83, N 3.93. Found: C 44.39, H 2.87, N 3.94. X-ray quality crystals were grown by slow evaporation of an acetone, methanol, and toluene solution.

Preparation of [Mn(hfacac)$_2$(1,3-bpyp)]$_2$·(Ph-CH$_2$-Ph) (11). Slow evaporation of an acetone/methanol solution of 37.9 mg (0.191 mmol) of **1** and 98.6 mg (0.188 mmol) of **2** in the presence of **4** gave 130.8 mg (93%; yellow solid) of **11**. Calculated for $Mn_2C_{59}H_{44}N_4O_8F_{24}$: C 47.15, H 2.95, N 3.73. Found: C 47.11, H 2.94, N 3.75. X-ray quality crystals were grown by slow evaporation of an acetone, hexanes, and diphenylmethane solution.

Preparation of [Mn(hfacac)$_2$(1,3-bpyp)]$_2$·(*cis*-stilbene) (12). Slow evaporation of an acetone/methanol solution of 36.2 mg (0.183 mmol) of **1** and 96.4 mg (0.184 mmol) of **2** in the presence of **5** gave 104.9 mg (76%; yellow solid) of **12**. Calculated for $Mn_2C_{60}H_{44}N_4O_8F_{24}$: C 47.57, H 2.93, N 3.70. Found: C 47.82, H 2.89, N 3.74. X-ray quality crystals were grown by slow evaporation of an acetone, methanol, hexanes, and *cis*-stilbene solution.

Preparation of [Mn(hfacac)$_2$(1,3-bpyp)]$_n$·*n*[Ph-(CH$_2$)$_3$-Ph] (13). Slow evaporation of an acetone/methanol solution of 46.0 mg (0.232 mmol) of **1** and 120.9 mg (0.231 mmol) of **2** in the presence of **6** gave 166.5 mg (84%; brown solid) of **13**. Calculated for $MnC_{38}H_{32}N_2O_4F_{12}$: C 52.85, H 3.73, N 3.24. Found: C 53.96, H 3.83, N 3.25. NOTE: elemental analysis is slightly off due to difficulties in removing all of the nonlattice **6** without also potentially removing it from its guest position in the lattice. X-ray quality crystals were grown by slow evaporation of an acetone, hexanes, 1,3-diphenylpropane, and water biphase mixture.

Preparation of [Mn(hfacac)$_2$(1,3-bpyp)]$_2$·(Ph-CH$_2$OH) (14). Slow evaporation of an acetone/hexanes solution of 60.3 mg (0.304 mmol) of **1** and 159.2 mg (0.304 mmol) of **2** in the presence of **7** gave 203.4 mg (93%; yellow solid) of **14**. Calculated for $Mn_2C_{53}H_{40}N_4O_9F_{24}$: C 44.12, H 2.79, N 3.88. Found: C 43.92, H 2.89, N 3.93. X-ray quality crystals were grown by slow evaporation of a methanol, acetone, and benzyl alcohol solution.

Preparation of [Mn(hfacac)$_2$(1,3-bpyp)]$_2$·2(nitrobenzene) (15). Slow evaporation of an acetone/hexanes solution of 61.17 mg (0.309 mmol) of **1** and 161.4 mg (0.309 mmol) of **2** in the presence of **8** gave 239.0 mg (97%; yellow solid) of **15**. Calculated for $Mn_2C_{58}H_{42}N_6O_{12}F_{24}$: C 44.07, H 2.68, N 5.32. Found: C 43.91, H 2.70, N 5.28. X-ray quality crystals were grown by slow evaporation of a methanol and nitrobenzene solution.

(7) (a) Yaghi, O. M.; Li, H.; Davis, C.; Richardson, D.; Groy, T. L. *Acc. Chem. Res.* **1998**, *31*, 474−484. (b) Moon, M.; Kim, I.; Lah, M. S. *Inorg. Chem.* **2000**, *39*, 2710−2711.

(8) Biradha, K.; Fujita, M. *J. Chem. Soc., Dalton Trans.* **2000**, 1−6.

(9) (a) Biradha, K.; Domasevitch, K. V.; Moulton, B.; Seward, C.; Zaworotko, M. J. *J. Chem. Soc., Chem. Commun.* **1999**, 1327−1328. (b) Biradha, K.; Mondal, A.; Moulton, B.; Zaworotko, M. J. *J. Chem. Soc., Dalton Trans.* **2000**, 3837−3844.

(10) (a) Karasawa, S.; Sano, Y.; Akita, T.; Koga, N.; Itoh, T.; Iwamura, H.; Rabu, P.; Drillon, M. *J. Am. Chem. Soc.* **1998**, *120*, 10080−10087. (b) Görlitz, G.; Hayamizu, T.; Itaoh, T.; Matsuda, K.; Iwamura, H. *Inorg. Chem.* **1998**, *37*, 2083−2085. (c) Plater, M. J.; Foreman, M. R. St. J.; Slawin, A. M. Z. *Inorg. Chim. Acta* **2000**, *303*, 132−136.

(11) Calhorda, M. J. *J. Chem. Soc., Chem. Commun.* **2000**, 801−809 and references therein.

Table 1. Crystallographic Parameters for Compounds **10**−**16**

	10	**11**	**12**	**13**	**14**	**15**	**16**
formula	$C_{53}H_{40}F_{24}Mn_2N_4O_8$	$C_{59}H_{44}F_{24}Mn_2N_4O_8$	$C_{60}H_{44}F_{24}Mn_2N_4O_8$	$C_{38}H_{32}F_{12}MnN_2O_4$	$C_{53}H_{40}F_{24}Mn_2N_4O_9$	$C_{58}H_{42}F_{24}Mn_2N_6O_{12}$	$C_{60}H_{42}F_{24}Mn_2N_6O_8$
mol wt	1426.77	1502.86	1514.87	863.60	1442.77	1580.86	1540.88
T/K	200(1)	200(1)	200(1)	200(1)	200(1)	200(1)	200(1)
system	triclinic	monoclinic	triclinic	monoclinic	triclinic	triclinic	triclinic
space group	*P*$\bar{1}$	*C*2/*m*	*P*$\bar{1}$	*Pn*	*P*$\bar{1}$	*P*$\bar{1}$	*P*$\bar{1}$
a/Å	10.1402(2)	13.3971(18)	13.6022(6)	14.2058(3)	10.0966(4)	14.0984(3)	14.0007(5)
b/Å	13.0837(3)	23.866(4)	15.4929(6)	9.9920(3)	13.1001(4)	14.6254(4)	14.7834(5)
c/Å	13.3685(3)	10.1985(16)	17.3102(5)	14.4406(3)	13.3725(4)	16.4762(3)	16.4656(4)
a/°	60.7325(15)	90	69.198(2)	90	61.1082(18)	80.7262(13)	80.8755(18)
β/deg	86.7121(13)	95.702(11)	72.195(2)	102.6740(10)	86.596(2)	78.7341(13)	78.1471(16)
γ/deg	80.4379(13)	90	73.270(2)	90	80.188(2)	89.5633(13)	89.4096(15)
V/Å^3	1525.13(6)	3244.7(8)	3180.2(2)	1999.82(8)	1525.39(9)	3287.30(13)	3292.27(18)
Z	1	2	2	2	1	2	2
μ/mm^{-1}	0.541	0.513	0.524	0.426	0.543	0.516	0.508
no. of measd reflcns	12547	4615	20985	8726	8813	21616	21699
no. of unique reflcns	8331	2796	14066	8726	5267	14435	14557
R(int)	0.0194	0.0543	0.0311	0.0000	0.0317	0.0268	0.0278
*R*1 ($I > 2\sigma(I)$)	0.0528	0.0800	0.0547	0.0497	0.0743	0.0612	0.0532
*wR*2 (on F^2, all data)	0.1290	0.2240	0.1288	0.1208	0.2110	0.1726	0.1312
GOF	1.012	1.046	1.009	1.055	1.095	1.029	1.012

Preparation of [Mn(hfacac)$_2$(1,3-bpyp)]$_2$·2(cyanobenzene) (16). Slow evaporation of an acetone/hexanes solution of 59.84 mg (0.302 mmol) of **1** and 157.9 mg (0.302 mmol) of **2** in the presence of **9** gave 191.6 mg (82%; yellow solid) of **16**. X-ray quality crystals were grown by slow evaporation of an acetone, methanol, and cyanobenzene solution.

Crystal Structure Determination. Single-crystal X-ray diffraction data for all the compounds were collected on a Nonius KappaCCD diffractometer equipped with Mo Kα radiation (λ = 0.71073 Å). The data collection was carried out at 200(1) K. Data were corrected for absorption by using the DENZO-SMN[12] program. The structure was solved by a combination of direct methods and heavy atom method with SIR97.[13] For the final structural refinement SHELXL97[14] was used. All of the non-hydrogen atoms were refined with an anisotropic displacement coefficient. Hydrogen atoms were assigned isotropic displacement coefficients U(H) = 1.2U(C) or 1.5U(Cmethyl), and their coordinates were allowed to ride on their respective carbons with use of SHELXL97 (exception for the disordered diphenylmethane (**4**) in compound **11**, no hydrogen atoms were calculated for **4**). Pertinent crystallographic data are listed in Table 1.

Results and Discussion

Equimolar reactions of 4,4′-trimethylenedipyridine (**1**) and manganese corner **2** in the presence of a variety of guests led to the formation of three major solid-state products: (a) dimeric species of the general formula [Mn(hfacac)$_2$(1,3-bpyp)]$_2$·G with guests G = **3**−**5**, **7**; (b) dimeric species of the general formula [Mn(hfacac)$_2$(1,3-bpyp)]$_2$·2G with guests G = **8** and **9** ; and (c) a syndiotactic coordination polymer [Mn(hfacac)$_2$(1,3-bpyp)]$_n$·*n*G with G = **6**. All products are formed at the solvent−crystal interface and characterized by X-ray crystallography. An in-depth inspection of the resultant structures reveals insights into the weak interactions that differentiate between them, as discussed below.

Host−guest complex [Mn(hfacac)$_2$(1,3-bpyp)]$_2$·toluene (**10**) results when **1** and **2** are crystallized in the presence of toluene (**3**). In contrast to the known structure of the helical, polymeric [Mn(hfacac)$_2$(1,3-bpyp)]$_n$,[3c] **10** forms a dimeric cyclophane in the solid state with one toluene molecule enclathrated per supramolecular ring (Figure 1).

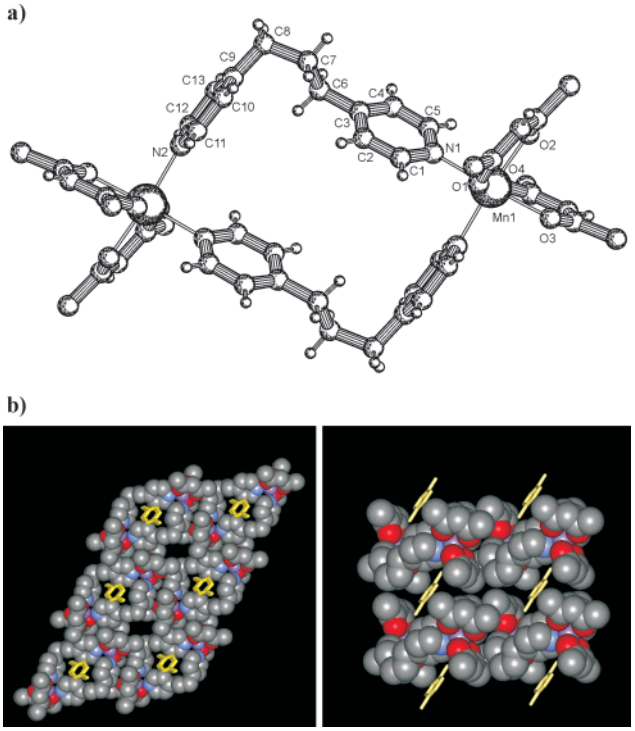

Figure 1. (a) PLUTON representation of **10**. Toluene molecule and fluorine atoms omitted for clarity. (b) Top and side views of the stacking diagram of **10** (CPK representation). Disordered toluene guest molecules are shown in yellow (stick illustration). Fluorine and proton atoms are omitted for clarity.

The coordination geometry about the manganese centers is pseudooctahedral with a cis orientation of the pyridine rings (N1−Mn1−N2′ = 90.4°). As expected, the Mn−O bonds trans to the nitrogens are slightly elongated (Mn1−O2 = 2.18 Å and Mn1−O3 = 2.20 Å) when compared to the axial Mn−O bonds (Mn1−O1 = 2.16 Å and Mn1−O4 = 2.14 Å). The diagonal Mn−Mn distance is 11.31 Å, while the shortest carbon−carbon (C2−C6′) cross-ring distance is 5.47 Å. These values are similar to other known dimeric rhomboids and ring systems.[15]

(12) Otwinowski, Z.; Minor, W. Processing of X-ray Diffraction Data Collected in Oscillation Mode. *Methods Enzymol*. **1997**, *276*, 307−326.

(13) SIR97 (Release 1.02), A program for automatic solution and refinement of crystal structure; Altomare, A., Burla, M. C., Camalli, M., Cascarano, G., Giacovazzo, C., Guagliardi, A., Moliteni, A. G. G., Polidori, G., Spagna, R.

(14) SHELX97 [Includes SHELXS97, SHELXL97, CIFTAB]; Programs for Crystal Structure Analysis (Release 97-2); Sheldrick, G. M.; University of Göttingen, Germany, 1997.

Table 2. Selected Bond Lengths and Bond Angles for Compounds **10** and **11**

compound **10**		compound **11**	
bond lengths (Å)			
Mn1−O1	2.1582(15)	Mn1−O1	2.137(3)
Mn1−O2	2.1818(16)	Mn1−O1′	2.137(3)
Mn1−O3	2.2006(16)	Mn1−O2	2.200(4)
Mn1−O4	2.1441(15)	Mn1−O2′	2.200(4)
Mn1−N1	2.2477(19)	Mn1−N1	2.262(5)
Mn1−N2′	2.2395(19)	Mn1−N1′	2.262(5)
bond angles (deg)			
N1−Mn1−N2′	90.44(7)	N1−Mn1−N1′	96.9(2)
N1−Mn1−O3	166.39(6)	N1′-Mn1−O2	165.37(15)
N2′-Mn1−O2	165.53(6)	N1−Mn1−O1	91.51(16)
O2−Mn1−O4	96.08(6)	N1−Mn1−O2	91.72(16)
O1−Mn1−O3	103.00(6)	O1−Mn1−O2	80.95(14)
C3−C6−C7	113.2(2)	O1−Mn1−O2′	100.75(14)
C6−C7−C8	112.5(2)	C8−C11−C12	109.4(5)
C7−C8−C9	111.1(2)	C11−C12−C11′	114.7(7)

Due to the flexibility of ligand **1**, it can adopt several conformations, such as *TT*, *TG*, *GG*, and *GG′* (relative orientations of the CH_2 groups, trans = *T*, gauche = *G*).[16] In this instance, coordinated ligand **1** adopts the *TG* orientation in the solid state. Other selected structural features of **10** are presented in Table 2.

These neutral macrocycles stack parallel to the *a*-axis, with an Mn−Mn distance between each cyclophane of 10.14 Å. This also corresponds to the length of the unit cell. The manganese rings form grooves in which the toluene molecules reside. In sitting on the crystallographic inversion center, the toluene is disordered in both possible orientations.

We assume that the dimeric structure results over the polymeric helix[3c] seen in the absence of a clathrate due to the formation of hydrophobic, inter-sheet pockets that envelop the nonpolar toluene as the crystal grows (Figure 2). Similar interactions have been noted for cyclodextrins and their host−guest complexes.[17]

In addition to the hydrophobic interactions, a close examination of the crystal structure reveals the presence of a C−H···π interaction between the toluene molecule and the pyridine moiety. The shortest C−H distance (2.80 Å) clearly lies in the range of a typical association of this sort,[18] with a 79.2° dihedral angle between the pyridine unit and toluene template. In addition, multiple weak interactions of a similar type exist between the alkyl chain protons and the toluene, where the shortest $C_{aromatic}-H_{alkyl}$ distance is 3.23 Å. It is likely the sum total of all of these weak forces (C−H···π/hydrophobic) that allows for the transformation of the structure from infinite polymer to closed dimeric system.

The assembly of **1** and **2** can also be templated by diphenylmethane (**4**), yielding $[Mn(hfacac)_2(1,3\text{-bpyp})]_2$·diphenylmethane (**11**). In contrast to **10**, the 1,3-bpyp ligand adopts a *TT* conformation, which leads to a larger internal cavity (Mn1−Mn1′ = 12.02 Å; C12−C12′ = 7.50 Å; Figure 3a). As a further consequence of this conformational change, the overall shape of the macrocycle in **11** is square-like, as opposed to the rectangular form seen in complex **10**.

(15) Schmitz, M.; Leininger, S.; Fan, J.; Arif, A. M.; Stang, P. J. *Organometallics* **1999**, *18*, 4817−4824 and references therein.
(16) Carlucci, L.; Ciani, G.; v. Gudenberg, D. W.; Proserpio, D. M. *Inorg. Chem.* **1997**, *36*, 3812−3813.
(17) Harada, A.; Takahashi, S. *J. Chem. Soc., Chem. Commun.* **1988**, 1352−1353.
(18) Madhavi, N. N. L.; Katz, A. K.; Carrell, H. L.; Nangia, A.; Desiraju, G. R. *J. Chem. Soc., Chem. Commun.* **1997**, 1953−1954.

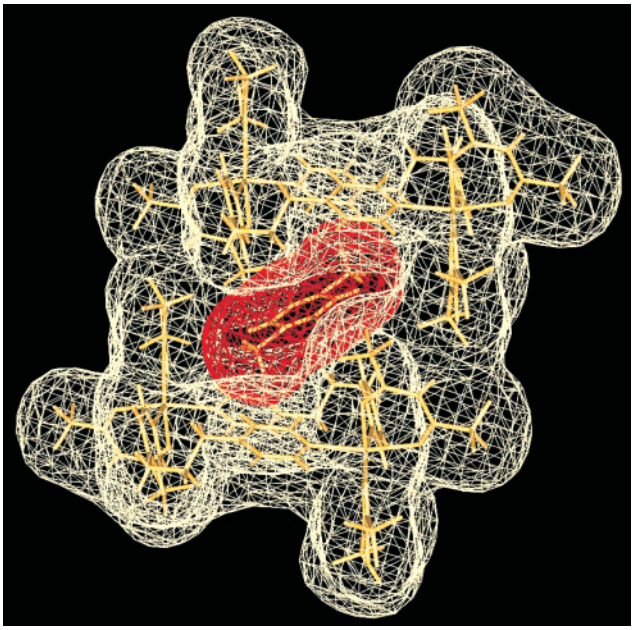

Figure 2. Representation of the van der Waals surfaces of the hydrophobic pocket formed by two macrocycles and its included toluene.

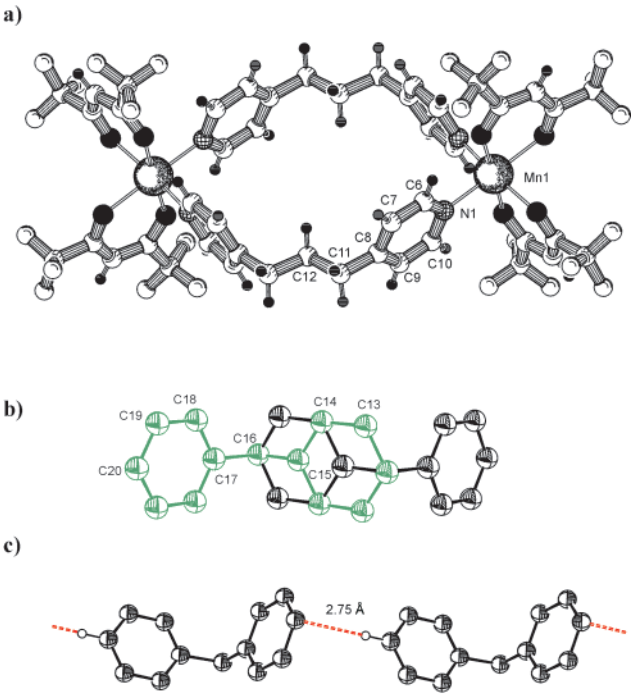

Figure 3. (a) PLUTON representation of the macrocycle portion of **11**. (b) ORTEP plot of diphenylmethane guest in **11** showing the disorder. (c) Portion of a zigzag, guest−guest chain in **11** formed via edge-to-face interactions between diphenylmethane molecules A and A′ (ORTEP plot).

As anticipated, the Mn−O bonds trans to the pyridyl moieties are again stretched (Mn1−O2 = 2.20 Å) when compared to those which are cis (Mn1−O1 = 2.14 Å). The Mn1−N1 bond distance (2.26 Å) lies in the expected range, while the nitrogen−manganese−nitrogen angle is enlarged to 96.9° (Table 2). Similar to **10**, the cyclophanes stack along the *c*-axis, with an inter-sheet distance of 10.2 Å.

Compound **11** crystallizes in the centrosymmetric space group $C2/_m$, generating a pseudodisorder in the noncentrosymmetric guest molecules. This subsequently results in an average of two

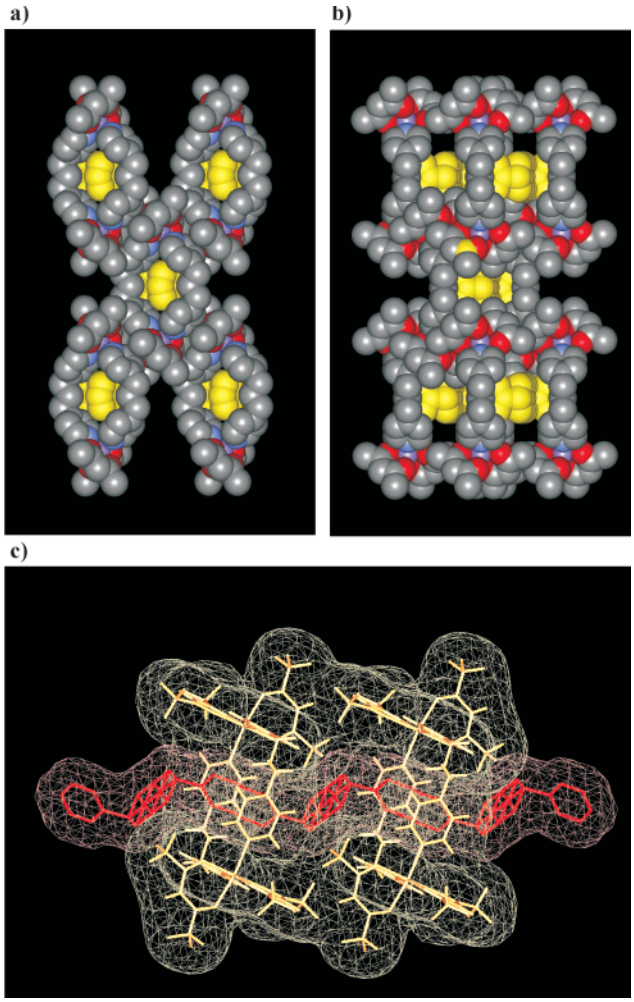

Figure 4. (a) Top and (b) side views of the stacking diagram of **11** (guest molecules shown in yellow). Fluorine and proton atoms are omitted for clarity. (c) van der Waals surfaces of **11** (guest molecules shown in red).

distinct clathrate orientations in the unit cell, as shown in Figure 3b. This disorder is most reasonably interpreted as each orientation existing as a separate entity and occupying a different position in the overall lattice.

The included diphenylmethane molecules of a specific orientation form infinite, zigzag chains via strong edge-to-face C−H···π interactions with each other (p-$H_{moleculeA}$−p-$C_{moleculeA'}$ = 2.75 Å; centroid$_{moleculeA}$−p-H $_{moleculeA}$−$C_{moleculeA'}$ = 175°; Figure 3c). These chains are aligned parallel to one another as they snake through the channels of the main framework (Figure 4). In essence, the stacking of the cyclophane systems in **11** thus provides a matrix for the highly directed crystallization of diphenylmethane. Similar phenomena were recently reported in which infinite metal-based networks act as media for the crystallization of noncovalent guest networks.[8,9]

Interestingly, no significant intermolecular contacts exist between diphenylmethane (**4**) and the framework (closest C−C distances are in the range of 3.71−3.82 Å). Furthermore, template **4** adopts an almost perfect C_{2v} conformation, as indicated by a C17−C16−C15 angle of 110.5° and dihedral angles (F_A and F_B) of 86.6° and 88.0°, respectively. This observation corresponds to previously reported ground-state calculations for diphenylmethane in the gas phase [$F_A = F_B$ = 90.0°; angle(C_{ring}−CH_2−C_{ring}) = 110.9°][19] and provides additional evidence for the absence of effective intermolecular interactions between **4** and the ring system.

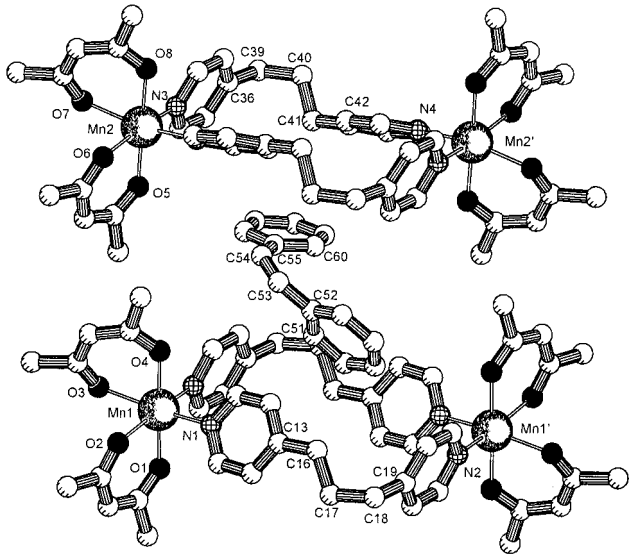

Figure 5. PLUTON representation of host−guest complex **12**, showing two conformationally distinct macrocycles and one *cis*-stilbene molecule. Proton and fluorine atoms are omitted for clarity.

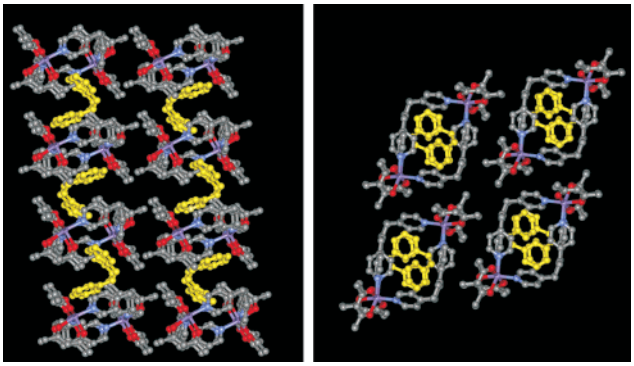

Figure 6. Side and top views of the stacking seen in **12** (ball-and-stick representation).

When *cis*-stilbene (**5**) is employed as a template in the crystallization of the metal−ligand system **1**/**2**, a host−guest clathrate [Mn(hfacac)$_2$(1,3-bpyp)]$_2$·*cis*-stilbene (**12**) results.

Similar to toluene complex **10**, the macrocycles in **12** exhibit an overall rectangular shape. Despite this likeness, however, the asymmetric unit of **12** consists of two independent manganese centers, two 1,3-bpyp ligands, and one complete *cis*-stilbene molecule, generating two individual and distinct ring systems in the crystal lattice. With a 6.6° angle between the best-fit planes of both cyclophanes, these two separate macrocycles are slightly tilted with respect to one another (Figure 5). This tilt results in an AB-type stacking (Figure 6), with two different inter-ring manganese−manganese distances (Mn1−Mn2 = 9.25 Å; Mn1′−Mn2′ = 9.44 Å; Mn2′−Mn1 = 9.25 Å; Mn2−Mn1′ = 9.44 Å). The metal−oxygen and metal−nitrogen bond distances and angles for the distorted octahedral centers of both dimers in **12** fall within the expected ranges (Table 3).

The first cyclophane in **12** shows a significant twisting of two of its four pyridyl moieties, with a torsion angle of 20.4° (N3−Mn2−N4′−C45′). In most cases, this torsion angle would lie between 60° and 90°. We believe that this deformation is a function of the many C−H···π interactions seen between the twisted pyridyl rings and one-half of the included *cis*-stilbene (aromatic as well as olefinic H−π contacts; Figure 7).

(19) Barnes, J. C.; Paton, J. D.; Damewood, J. R.; Mislow, K. *J. Org. Chem.* **1981**, *46*, 4975−4979.

Table 3. Selected Bond Lengths [Å] and Angles [deg] for **12** and **13**

compound **12**				compound **13**	
bond lengths (Å)					
Mn1−O1	2.1501(18)	Mn2−O5	2.1564(18)	Mn1−O1	2.174(2)
Mn1−O2	2.199(2)	Mn2−O6	2.171(2)	Mn1−O2	2.192(2)
Mn1−O3	2.224(2)	Mn2−O7	2.218(2)	Mn1−O3	2.182(2)
Mn1−O4	2.1513(18)	Mn2−O8	2.1507(18)	Mn1−O4	2.149(2)
Mn1−N1	2.252(2)	Mn2−N3	2.222(2)	Mn1−N1	2.222(3)
Mn1−N2′	2.253(2)	Mn2−N4′	2.246(2)	Mn1−N2′	2.214(3)
bond angles (deg)					
N1−Mn1−N2′	99.55(9)	N3−Mn2−N4′	95.63(9)	N1−Mn1−N2′	89.32(9)
N1−Mn1−O3	159.87(8)	N3−Mn2−O6	167.38(8)	N1−Mn1−O2	172.39(10)
N2′-Mn1−O2	165.79(8)	N4′-Mn2−O7	158.28(8)	N2′-Mn1−O3	178.85(11)
O2−Mn1−O4	99.21(8)	O6−Mn2−O8	98.12(8)	O2−Mn1−O4	90.97(10)
O1−Mn1−O3	100.14(7)	O5−Mn2−O7	100.81(7)	O1−Mn1−O3	86.92(9)
C13−C16−C17	117.6(2)	C36−C39−C40	110.7(2)	C13−C16−C17	109.7(3)
C16−C17−C18	112.0 (2)	C39−C40−C41	112.5 (2)	C16−C17−C18	112.9 (3)
C17−C18−C19	112.0 (3)	C40−C41−C42	111.7 (2)	C17−C18−C19	114.8 (3)

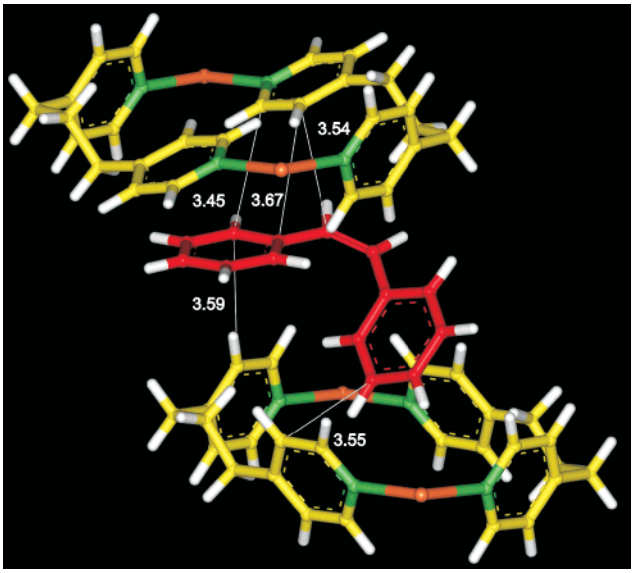

Figure 7. Contacts between *cis*-stilbene and a host pocket comprising the two independent macrocycles in **12** (ball-and-stick representation). Hfacac ligands are omitted for clarity.

In contrast, the second macrocycle in **12**, which shows no noteworthy distortion of any of its coordinated pyridine subunits, has only a single C−H···π interaction with the remaining portion of the enclathrated guest (Figure 7). The combination of these two phenomena also notably shapes the conformation of the *cis*-stilbene, when compared with the previously reported gas-phase, electron-diffaction study of the pure material.[20] The most significant difference is the torsion angle C53−C54−C55−C60 = 29.8°, which is reduced by about 13.4° relative to the gas state, and corresponds to the part of the *cis*-stilbene with the many C−H···π contacts. The second torsion angle (C51−C52−C53−C54 = 46.9°), which is influenced by only one host−guest interaction, is similar to that of the pure substance.

Interestingly, no intermolecular, clathrate−clathrate contacts of the sort seen in **11** are found in **12**. Accordingly, each *cis*-stilbene is isolated and can be viewed as occupying a complementary pocket consisting of two independent manganese rings that forms as the lattice evolves. The unsymmetrical host−guest interactions present force this pocket to be more compact and of different shape than that seen in **10**.

When 1,3-diphenylpropane (**6**), the next highest diphenyl derivative, is used as a guest in the crystallization of **1**/**2**, a dramatic change in the solid-state structure of **13** occurs. As opposed to the dimeric systems described previously, **13** crystallizes as an infinite coordination polymer with a metal−ligand−clathrate ratio of 1:1:1 ($[Mn(hfacac)_2(1,3\text{-bpyp})]_n \cdot n$**6**; Figure 8).

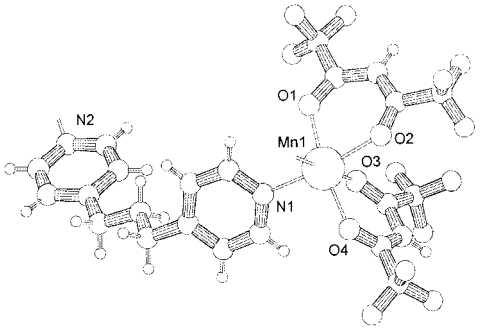

Figure 8. PLUTON representation of the asymmetric unit of **13** (the disordered diphenylpropane molecule is omitted for clarity).

The bond lengths and angles found for **13** are comparable to those of macrocycles **10**−**12** (Tables 2 and 3), while the shortest metal−metal distance in a given polymeric chain is 13.10 Å. This is slightly longer than the cross-ring distances for the closed systems. Similar to **11**, the 1,3-bpyp ligand adopts a *TT* conformation, allowing for the connection of metal centers of opposite chirality and subsequently leading to the formation of a wedge-shaped, syndiotactic polymer (Figure 9). The distance between metal centers of the same chirality is 22.37 Å; this quantity resembles the "pitch height" found for helical polymers.

We reason that the size of the guest molecule plays a crucial role in the formation of the polymer over the closed macrocycles. Both phenyl rings of **6** show a well-defined C−H···π interaction [edge-to-face, $d(\text{phenyl}_{\text{centroid}}-\text{H}_{\text{pyridine}}) = 2.86$ and 2.99 Å] with the pyridine units of the host. In contrast to all of the preceding cases, however, this interaction occurs between the pyridine moieties of a single ligand **1** and both phenyl rings of a single guest molecule, resulting in a *TT* conformation for **6** (the central CH_2 group is disordered). This unique, size-induced situation precludes the assembly of a dimeric ring system (Figure 9a).

Even though the clathrate occupies most of the volume in the trough-shaped framework, a partial interpenetration of the chains takes place and gives rise to a highly ordered structure for **13** (Figure 9b). No such interpenetration is seen between adjacent sheets (Figure 9c), which are oriented toward each other in such a way that the chirality of the metal center changes when moving from one layer to the next (Figure 9d).

(20) Traetteberg, M.; Frantsen, E. B. *J. Mol. Struct.* **1975**, *26*, 69−76.

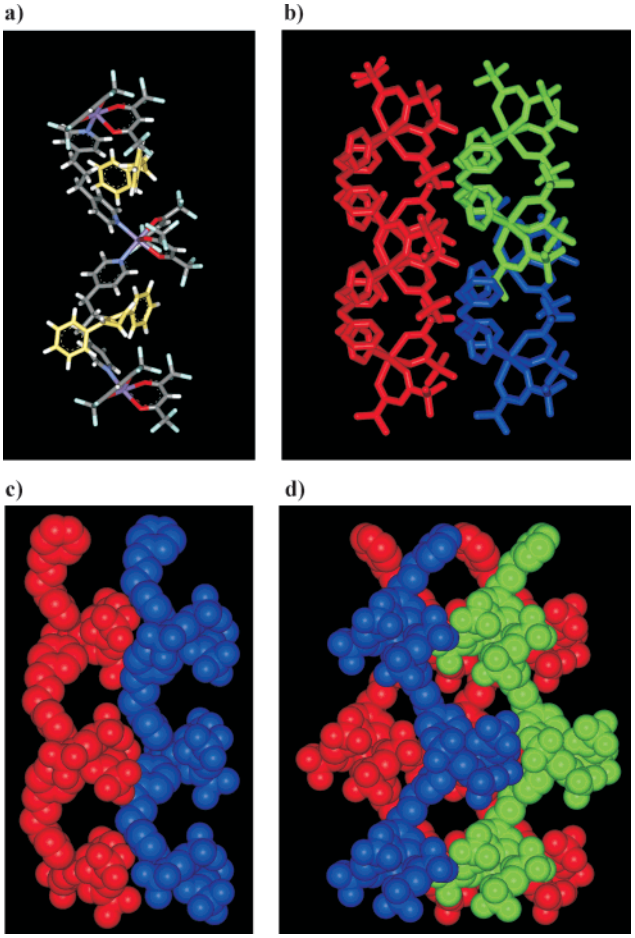

Figure 9. (a) Portion of the syndiotactic polymer **13**. Guest molecules are yellow (stick representation). (b) View along the polymeric axis of **13**. Guest molecules are omitted (stick representation). (c) Side view of two sheets (CPK representation). (d) Two layers of **13**, showing the change of chirality (CPK representation).

To add a further "linking" motif, the guests benzyl alcohol (**7**), nitrobenzene (**8**), and cyanobenzene (**9**) are exploited in the reaction of **1** and **2**. These clathrates have the potential for classical and/or nonclassical hydrogen bonding in addition to the π and van der Waals interactions already seen for the purely nonpolar systems.

Despite the hydrogen-bonding capabilities of benzyl alcohol (**7**), the resulting host−guest complex **14** is isostructural to toluene system **10** and shows no classical H-bonds at all. In this case, the added functionality is overwhelmed by the large number of host−guest interactions generated by the hydrophobic pocket.

When **1** and **2** are exposed to nitrobenzene (**8**), which has a permanent dipole and thus a higher capacity for nonclassical hydrogen bonds, the complex $[Mn(hfacac)_2(1,3\text{-bpyp})]_2\cdot$2nitrobenzene (**15**) is formed (Figure 10). The stoichiometry for the ensuing product consists of 1 equiv each of ligand **1**, corner **2**, and guest **8**.

The skeleton of **15** is quite similar to that found for **11** in terms of both its shape and dimensions. For instance, the dipyridyl unit **1** also adopts a *TT* conformation, and the cross-ring distances Mn1−Mn2 (12.36 Å) and C17−C30 (7.08 Å) are comparable. As seen previously, all of the bond angles and lengths lie in the typical range for pseudooctahedral coordination about manganese centers of this type (Table 4).

The nitrobenzene molecules are positioned above and below the plane of the ring in an ordered fashion. While disorder is

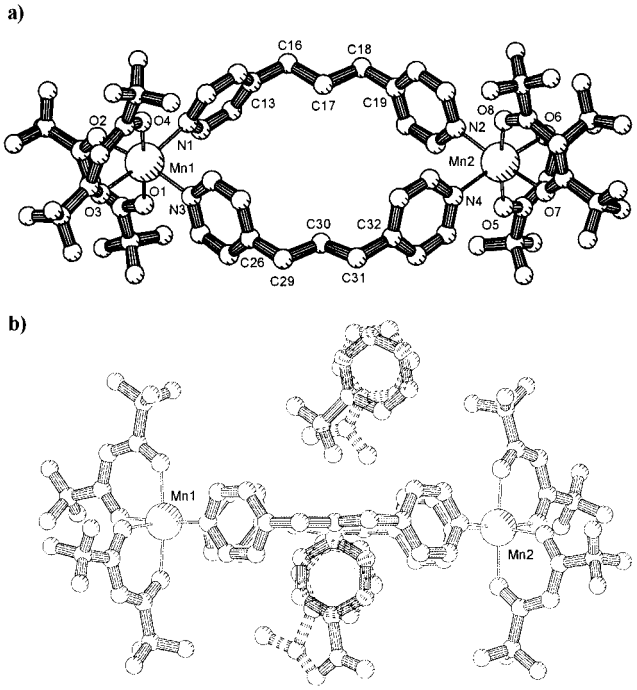

Figure 10. PLUTON representation (a) main skeleton of **15** (protons and guest molecules omitted for clarity). (b) Side view of the asymmetric unit of **15** showing the orientation of the nitrobenzene relative to the ring system (protons omitted).

Table 4. Selected Bond Lengths and Angles for Compound **15**

bond lengths (Å)		bond angles (deg)	
Mn1−O1	2.158 (2)	N1−Mn1−N3	91.71 (9)
Mn1−O2	2.172 (2)	N2−Mn2−N4	89.43 (9)
Mn1−O3	2.221 (2)	N1−Mn1−O3	170.90 (9)
Mn1−O4	2.153 (2)	N3−Mn1−O2	171.31 (9)
Mn1−N1	2.266 (2)	N2−Mn2−O7	176.01 (8)
Mn1−N3	2.245 (2)	N4−Mn2−O6	172.06 (9)
Mn2−O5	2.141 (2)	O1−Mn1−O3	94.16 (8)
Mn2−O6	2.194 (2)	O2−Mn1−O4	95.63 (8)
Mn2−O7	2.190 (2)	O5−Mn2−O7	89.37 (8)
Mn2−O8	2.146 (2)	O6−Mn2−O8	94.83 (8)
Mn2−N2	2.252 (3)	O4−Mn1−N3	92.15 (9)
Mn2−N4	2.250 (3)	O5−Mn2−N2	93.94 (9)

seen in the guests themselves, the overall directionality is always maintained (Figure 10b). We believe that this results from weak hydrogen bonding[8,11] between the included clathrate molecules in which the oxygen atoms of each nitrobenzene interact with the aromatic protons of the next nitrobenzene (Figure 11a). These C−H···O linkages range from 2.1 to 2.6 Å, allowing for the formation of infinite guest columns that string through the channels of *b*-axis stacked macrocycles (Mn−Mn stacking distance = 14.6 Å).

Despite the directionality in any given column, the overall crystal has no macroscopic dipole moment due to the fact that every chain has an oppositely directed counterpart (Figure 11b). With no host−guest interactions evident, **15** shows the same type of matrix behavior as seen in **11**, except in this case, it is based upon nonclassical hydrogen bonding as opposed to edge-to-face C−H···π interactions.

Cyanobenzene **9** templates the solid-state product of the reaction of **1** and **2** in a manner identical with that for nitrobenzene (**8**). This leads to the formation of a host−guest complex $[Mn(hfacac)_2(1,3\text{-bpyp})]_2\cdot$2cyanobenzene (**16**) (Figure 12) that is isostructural to **15**.

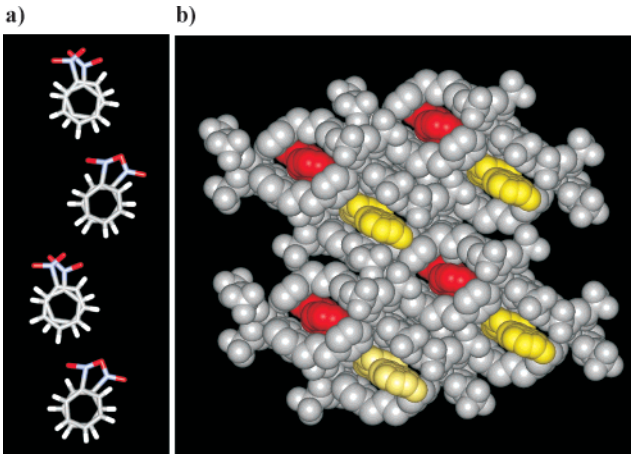

Figure 11. (a) An example of the one-dimensional columns formed by the disordered nitrobenzene guests (stick representation). (b) Framework (grey) of **15** with included, oppositely directed nitrobenzene columns (red and yellow) (CPK model; protons are omitted for clarity).

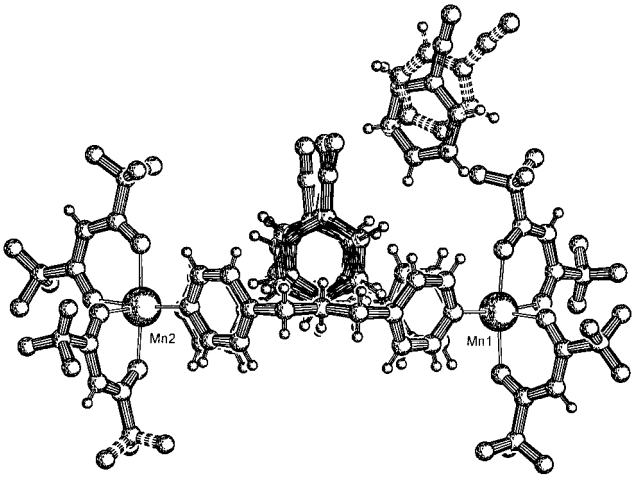

Figure 12. PLUTON representation of the asymmetric unit of **16** showing the higher degree of disorder for one of the cyanobenzenes and their relative orientation to the ring system and each other (disordered fluorine atoms are omitted for clarity).

While one cyanobenzene molecule shows a higher degree of disorder than the other, the overall directionality of the guest molecules is still preserved. As in **15**, columns form through nonclassical hydrogen bonding between the included solvent molecules (Figure 13). In this instance, the interaction occurs as a C−H···N linkage between the cyano nitrogen of one cyanobenzene and the phenyl protons of the adjacent guest. As is the case for **15**, no macroscopic dipole moment is present in **16**.

To further improve our knowledge of these structures and allow for potential, future predictability, competition experiments can be undertaken in which guest selectivity is probed. The first, most logical of these is matching the two solvents showing identical guest behavior, nitrobenzene (**8**) and cyanobenzene (**9**). Both of these clathrates yield isostructural metal−ligand−guest complexes, **15** and **16**, respectively, and exhibit no interactions with the host framework. Instead, they possess guest−guest, nonclassical hydrogen bonding that leads to the formation of infinite solvent columns in the overall crystal lattice. When the metal−ligand system **1**/**2** is crystallized in the presence of equimolar amounts of both solvents **8** and **9**, only the nitrobenzene superstructure **15** forms.[21] This preference toward nitrobenzene may be explained by the fact that lattice

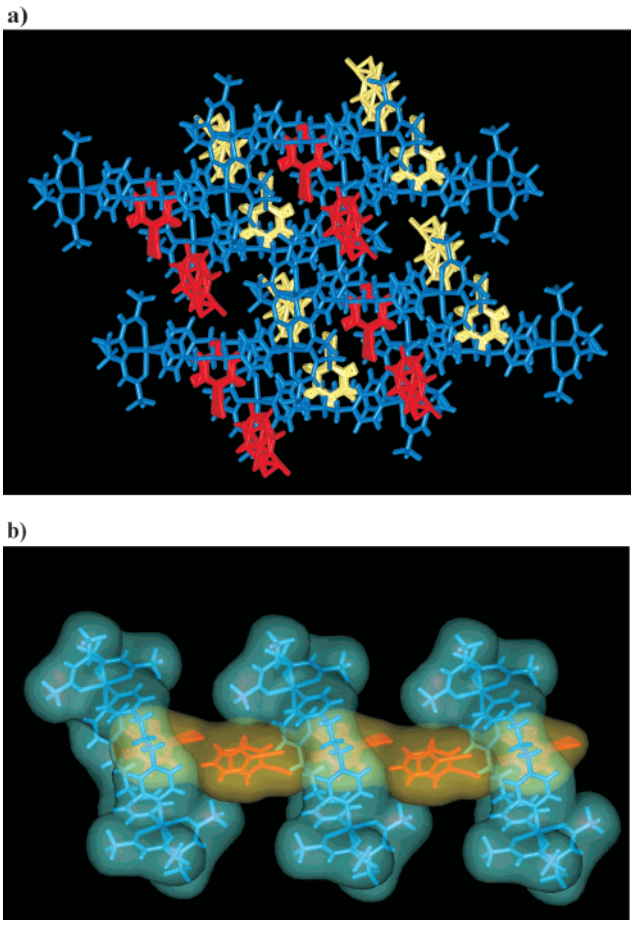

Figure 13. (a) Framework (blue) of **16** with included, oppositely directed cyanobenzene columns (red and yellow) (stick representation). (b) An example of a one-dimensional column formed by the disordered cyanobenzene guests stringing through the cyclophanes of **16** (stick representation with van der Waals surfaces).

15 has a much lower calculated void space than **16** (0.7% vs 2.8%, respectively).[22] One must, of course, also consider the differing dipole moments between **8** and **9**, which could influence the outcome of the reaction.

A second, reasonable competition study involves discriminating between the toluene complex **10**, which consists of a myriad of hydrophobic host−guest interactions, and the nitrobenzene complex **15**, which comprises interguest C−H···O linkages. This trial therefore pits complexes with exclusively host−guest interactions, **10**, against those relying entirely upon guest−guest forces, **15**. Even with the higher void space found for toluene complex **10** versus nitrobenzene adduct **15** (1.6% and 0.7%, respectively), the toluene enclathrated material **10** is still the sole product in a similar competition experiment. This may be the result of the many weaker hydrophobic interactions present in **10** dominating the solitary, highly directed C−H···O "bonds" of **15**.

Conclusion

By reacting manganese corner unit **2** with flexible dipyridyl unit **1**, and thereby utilizing the nucleophilic subunits as essential, tunable components of the overall framework instead of merely "spacers", we are able to change a single metal−

(21) Guests **8** and **9** were equimolar relative to each other, but were in excess relative to the metal−ligand system **1**/**2**.

(22) PLATON program: Spek, A. L. *Acta Crystallogr., Sect. A* **1990**, *46*, 194−201.

ligand system from an infinite helix to both closed dinuclear macrocycles and a wedge-shaped, syndiotactic polymer. The molecular "information" that is lost by employing a less rigid ligand like **1** is compensated for by several simple organic templates that form a variety of weak intermolecular interactions between the guest molecules themselves and/or with the host. The overall crystal-topology of the resulting solid state assembly is found to be highly dependent upon these auxiliary forces, and competition experiments show that future predictability may be possible with further understanding. Furthermore, interpenetration is precluded to a large degree, or altogether in many instances, thereby allowing a potential path toward mesoporous materials. Moreover, the strategy that we present herein, where motifs other than the dative bonding of highly programmed, rigid subunits are exploited, may serve as a guide for the continued development of the field of inorganic crystal engineering.

Acknowledgment. This research was supported by the National Science Foundation (CHE-9818472) and the Alexander von Humboldt Foundation via a Feodor Lynen Fellowship for F. M. Tabellion. Furthermore, we are grateful to Prof. Myoung Soo Lah for his expertise in intermolecular interactions and void space calculations. Dedicated to Professor Michael Hanack on the occasion of his 70th birthday.

Supporting Information Available: Crystallographic data for **10**−**16** (CIF). This material is available free of charge via the Internet at http://pubs.acs.org.

JA0114310